

Delta ferrite formation and evolution during slab processing from an 80-ton industrial heat of AISI 304 austenitic stainless steel

<http://dx.doi.org/10.1590/0370-44672022760001>

Flávia Andressa Moreira dos Santos^{1,3}

<https://orcid.org/0000-0002-8589-7050>

Marcelo Aquino Martorano^{2,4}

<https://orcid.org/0000-0001-5163-3279>

Angelo Fernando Padilha^{2,5}

<https://orcid.org/0000-0002-5494-9137>

¹Aperam Inox Serviços Brasil Ltda
Campinas – São Paulo – Brasil

²Universidade de São Paulo – USP, Escola Politécnica,
Departamento de Engenharia Metalúrgica e de
Materiais, São Paulo - São Paulo - Brasil.

E-mails: ³flaviaams@alumni.usp.br, ⁴martoran@usp.br,
⁵padilha@usp.br

Abstract

Although delta ferrite is a very common phase in most austenitic stainless steels, studies about its formation and evolution during slab processing from industrial heats of tens of tons are scarce. The main objective of this research is to study the evolution of delta ferrite (quantity, chemical composition, morphology, and distribution) along the production route from the cast slab to the coil of an industrial heat of 80 tons of 304 stainless steel. Samples were extracted after the following processing steps: continuous casting, first and second hot-rolling pass, and solution-heat-treating, arriving at the final commercial condition. Sample analyses were carried out with several complementary microstructural characterization techniques: optical microscopy, scanning electron microscopy with energy dispersive spectroscopy (EDS), X-ray diffraction, and magnetic measurements of delta ferrite content (feritscope). Thermocalc® indicates that the present continuous cast slab solidifies according to the FA (ferrite-austenite) mode and the final microstructure should be completely austenitic in equilibrium conditions. Nevertheless, delta ferrite is detected along the processing steps, indicating that the steel is out of phase equilibrium. The ferrite content measured after solidification varies significantly across the as-cast slab thickness. Lower values are detected on the surfaces, followed by a gradual increase when moving into the slab, reaching a peak, and finally decreasing at the slab center. This pattern of delta ferrite content is named “M type” distribution. The average content of delta ferrite decreases after each subsequent processing step, namely the two hot-rolling passes and the solution heat-treating.

Keywords: austenitic stainless steel, delta ferrite, solidification, microstructure.

1. Introduction

Austenitic stainless steels have been commercially available since the second decade of the 20th century. They are still essential and almost irreplaceable in numerous applications owing to their good cost-benefit value (Padilha *et al.*, 2007). Among all stainless-steel grades, austenitic grades account for about ¾ of the world production. A large group of the austenitic grades are not completely austenitic in their working conditions, displaying amounts of retained delta ferrite (δ) between 0.5 and 5(vol)% even after undergoing solution heat-treating (Martorano *et al.*, 2012). Delta ferrite precipitates during solidification (Baldissin *et al.*, 2007) and its content, morphology, and distribution change during thermomechanical processing (Rezayat *et al.*, 2016).

The precipitation and growth/dissolution of the delta ferrite essentially depends on the steel chemical composition, the conditions during solidification (Martorano *et al.*, 2012), such as the solidification rate, and subsequent thermomechanical processing (Rezayat *et al.*, 2016). The amount and morphology of delta ferrite affects the steel hot formability, weldability, mechanical and corrosion properties (Padilha *et al.*, 2007). Consequently, studies about the solidification, growth, and dissolution of delta ferrite in this steel grade are particularly important.

Among stainless steels, AISI 304 is one of the oldest and most used in practical applications. Its base composition, referred to as V2A, was patented in 1912 by the German company

Krupp, which in 1914 delivered for the first time 18 tons of this steel to the German chemical company BASF (Padilha, 2002). The 304 stainless steel is currently commercialized as sheets or coils, rolled from a continuously cast slab. There are numerous studies about the formation of delta ferrite in the AISI 304 stainless steel, but very few examined samples extracted from industrial heats of tens of tons (Kim *et al.*, 1995; Kim *et al.*, 2003; Fukumoto *et al.*, 2012; Fu *et al.*, 2012). Furthermore, very few studies considered all processing steps from solidification up to the semi-finished product.

The 3XX grades of stainless steels can solidify according to the following two modes:

- FA: $L \rightarrow L + \delta$ (ferrite) $\rightarrow L + \delta + \gamma \rightarrow \gamma + \delta$
- AF: $L \rightarrow L + \gamma$ (austenite) $\rightarrow L + \gamma + \delta \rightarrow \gamma + \delta$

At larger solidification rates and lower ratios of Cr equivalent to Ni equivalent (Cr_{eq}/Ni_{eq}), the solidification

mode AF occurs more frequently than mode FA (Fu *et al.*, 2012). Among several expressions to calculate Cr_{eq} and

Ni_{eq} , those proposed by Suutala and co-authors are frequently adopted and are given below (Suutala *et al.*, 1980):

$$Cr_{eq} = Cr + Mo + 1.5 Si + 0.5 Nb \quad (1)$$

$$Ni_{eq} = Ni + 30 C + 0.5 Mn \quad (2)$$

The main objective of the present research was to study the evolution of delta ferrite in samples extracted along the pro-

duction route (from slab to coil) of an industrial heat of 80 tons of the 304 stainless steel. Sample microstructures were characterized

with several complementary techniques to show the amount, chemical composition, morphology, and distribution of delta ferrite.

2. Materials and methods

The evolution of delta ferrite during the production route (continuous casting, hot-rolling, and solution heat-treating) from slab to coil of an industrial heat of

304 stainless steel of chemical composition (Table 1) compatible with the UNS S30400 alloy of the ASTM A420/ A420M (2018 revision) was studied. The microstructural

phases that should exist in the present as-cast slab were initially predicted as a function of temperature by the software package Thermocalc® (version TCFE7).

Table 1 – Chemical composition of the industrial cast slab studied in the present research.

C	Mn	Si	P	S	Cr	Nb	Ni	Mo	Cu	Co	N
0.037	1.16	0.46	0.03	0.001	17.61	0.0038	8.01	0.05	0.1058	0.099	0.0403

Samples were extracted for analyses after the following processing steps: (1) continuous casting (slab of 1290 mm width x 200 mm thickness); (2) first hot-rolling pass (1270 mm width x 28 mm thickness); (3) second hot-rolling pass (1270 mm width x 4 mm thickness); and (4) solution heat-treating and pickling. The locations of the 16 samples extracted from the continuously cast slab are given

in Figure 1. Five sets of three samples were selected at different distances from the slab center along its width. In each set, one sample was located at the slab surface and the others at two different distances from the surface, namely ¼ and ½ of the slab thickness. The delta ferrite content was measured along the whole slab thickness in sample “A”, located at an arbitrary position along the slab width. After the

first and second hot-rolling passes, seven equidistant samples were extracted along the plate/sheet width. After heat-treating, samples were also taken from 185, 410 and 635 mm from the sheet center. All samples extended along the whole plate/sheet thickness, analogous to sample “A” in Figure 1.

The microstructures of the samples were characterized with the following complementary techniques: optical

microscopy, scanning electron microscopy, X-ray diffraction, and the magnetic method to measure delta ferrite contents. Metallographic preparation of the samples consisted of grinding with silicon carbide papers up to grit 1000, followed by mechanical polishing with diamond pastes of 3 and 1 μm , and a final mechanical polishing with alumina suspension. Samples

were etched in a solution of 10 g of NaOH in 100 mL of H_2SO_4 to reveal and measure delta ferrite contents. Microstructures were observed with the optical microscope Leica Model DMRM, in which fractions of delta ferrite area were measured using the Buehler OmnimetTM software, and observed with the FEG Inspect F50 – FEI electron microscope. Delta ferrite and aus-

tenite were detected with X-ray diffraction in samples extracted from a distance to the surface between $\frac{1}{4}$ and $\frac{1}{2}$ of the slab thickness using a Philips X'Pert diffractometer with an angular step of 0.01° and Cu-K α radiation. A Fischer Feritscope model MP30E was used to measure the content of magnetic phase by the magnetic method with a minimum limit of 0.1 (vol) %.

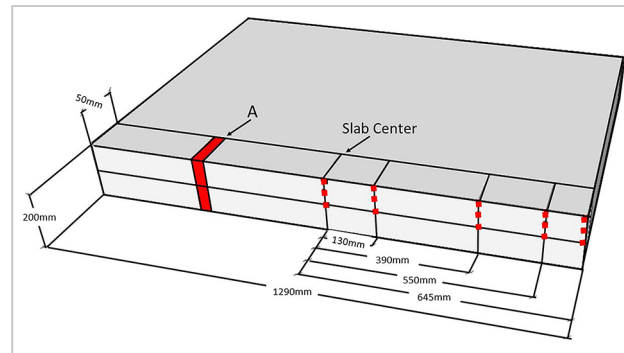


Figure 1 - Locations in the as-cast slab of the 16 samples extracted for analyses.

3. Results and discussion

Calculations of Cr_{eq} and Ni_{eq} using the expressions proposed by Suutala and co-authors (Eqs. (1) and (2)) for the composition in Table 1 gave $\text{Cr}_{\text{eq}}/\text{Ni}_{\text{eq}} = 1.89$, in the range between 1.5 and 2. In this range, solidification should occur according to the FA mode ($L \rightarrow L + \delta \rightarrow L + \delta + \gamma \rightarrow \gamma + \delta$), i.e., it begins with the formation of delta ferrite dendrites that partially transform to austenite by a peritectic reaction ($L + \delta \rightarrow \gamma$). After solidification, during cooling to room temperature, a subsequent solid-state transformation from ferrite to austenite ($\delta \rightarrow \gamma$) might give a completely austenitic microstructure, if the diffusion kinetics of elements is sufficiently high (Suutala et al., 1980; Rajasekhar et al., 1997). It is important to remember that these predic-

tions are based on many experimental observations in non-equilibrium conditions.

A Thermocalc[®] simulation in equilibrium conditions (lever rule) of the solidification sequence of the present 304 steel is given in Figure 2. This simulation shows that solidification begins at approximately 1460 °C with the formation of delta ferrite and that its volume fraction increases to 64.5% during cooling to about 1440 °C, with an increase of the concentration of austenite stabilizer elements in the liquid (Fredriksson, 1972; Okamoto et al., 1981). As temperature decreases even further, delta ferrite transforms to austenite according to the peritectic reaction $L + \delta \rightarrow \gamma$, causing a decrease in delta ferrite fraction to 57.2% at the

end of solidification, corresponding to an increase in the austenite fraction. This simulation in equilibrium conditions agrees with the non-equilibrium prediction of the FA solidification mode based on the ratio of $\text{Cr}_{\text{eq}}/\text{Ni}_{\text{eq}} = 1.89$. Solidification ends at 1427.5 °C and, during cooling to 1267.5 °C, calculations with Thermocalc[®] indicate that the retained delta ferrite completely transforms into austenite by a solid-state transformation ($\delta \rightarrow \gamma$). Consequently, the present 304 stainless steel should be completely austenitic in equilibrium conditions. Some phase transformations that could occur below 900 °C, such as the precipitation of M_{23}C_6 ($\text{M} = \text{Fe}, \text{Cr}$) and sigma-phase (Padilha & Rios, 2002), are not within the scope of the present study.

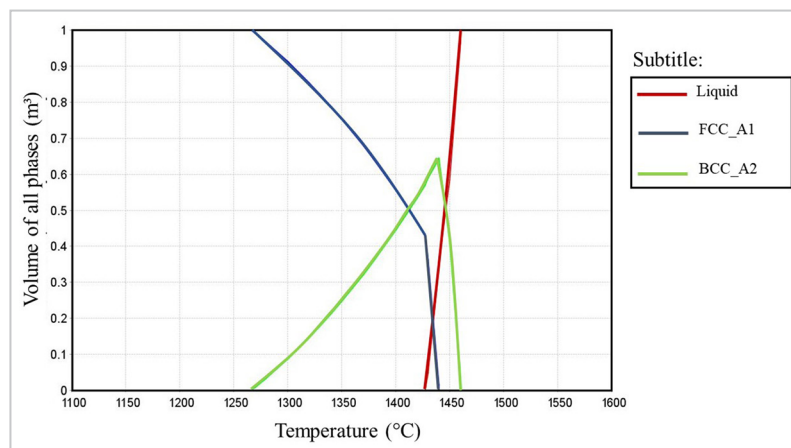


Figure 2 - Volume fractions of austenite (FCC_A1), delta ferrite (BCC_A2), and liquid as a function of temperature calculated with Thermocalc[®] (lever-rule) during solidification of the present 304 stainless steel (Table 1).

The microstructures observed in the optical microscope of the 15 samples (Figure 1) from the as-cast slab are presented in Figure 3. Retained delta ferrite embedded in an austenitic matrix is seen in all micrographs. The delta ferrite indicates the center of the arms of the initial dendritic structure. The existence of retained delta ferrite and austenite agrees with the predictions based on the ratio of $C_{r_{eq}}/Ni_{eq} = 1.89$ and with Thermocalc® simulations at the end of solidification. The existence of delta ferrite at room temperature, however, disagrees with the Thermocalc® calculations for cooling to 1100 °C, which predicts complete transformation of delta ferrite to austenite according to the solid-state transformation $\delta \rightarrow \gamma$. This discrepancy might indicate that the cooling rate during solidification and cooling to room temperature of the present slab is too high to allow enough diffusion of elements to complete the possible phase transformations.

As the distance to the surface of the samples increases (at surface, ¼ thickness, and ½ thickness), Figure 3 indicates a coarser dendritic structure of delta ferrite

(vermicular morphology) and a tendency towards a ferrite network. The samples at ½ thickness display some very clear regions and some porosity. This porosity is expected at the slab center, causing larger errors in delta ferrite measurements.

The volume fraction of delta ferrite measured with the magnetic method (feritscope) along the as-cast slab thickness in sample “A” (Figure 1) is shown in Figure 4, in excellent agreement with the results reported by Kim *et al.* (1995) for a similar slab. The delta ferrite content increases from both slab surfaces towards the center but begins to decrease at a distance of approximately 80 mm from each surface, reaching a minimum point at the slab center (“M Type pattern”). The standard deviation, calculated from ten measurements at each spot, increases towards the center probably owing to the increasing porosity. The present study confirms the so-called “M Type” ferrite distribution pattern observed by Kim *et al.* (1995) for industrial continuously cast slabs of stainless steels (Chen & Cheng, 2017; Zangar *et al.*, 2021).

When the chemical composition is

constant (i.e., absence of macrosegregation), the amount of delta ferrite depends on the dendrite arm spacing of the initial dendrites of delta ferrite and on the cooling rate during and after solidification. A decrease in dendrite arm spacing or a decrease in the cooling rate, which is inversely proportional to the diffusion distance defined as $\sqrt{(D t_L)}$ (where D is the diffusion coefficient of solute elements and t_L is the local solidification time), facilitates the diffusion of elements in the solid and accelerates the transformation of delta ferrite to austenite during solidification (peritectic) and cooling to room temperature (Dantzig & Rappaz, 2009). Kim *et al.* (1995) verified that the dendrite arm spacing increased sharply from the slab surface to its center and that the diffusion distance increased, reached a maximum, and decreases thereof. Therefore, these authors (Kim *et al.*, 1995) concluded that the increase in delta ferrite content from the surface into the slab was due to the prevailing effect of the increase in dendrite arm spacing, decreasing the diffusion flux, and consequently, the extent of the ferrite to austenite transformation.

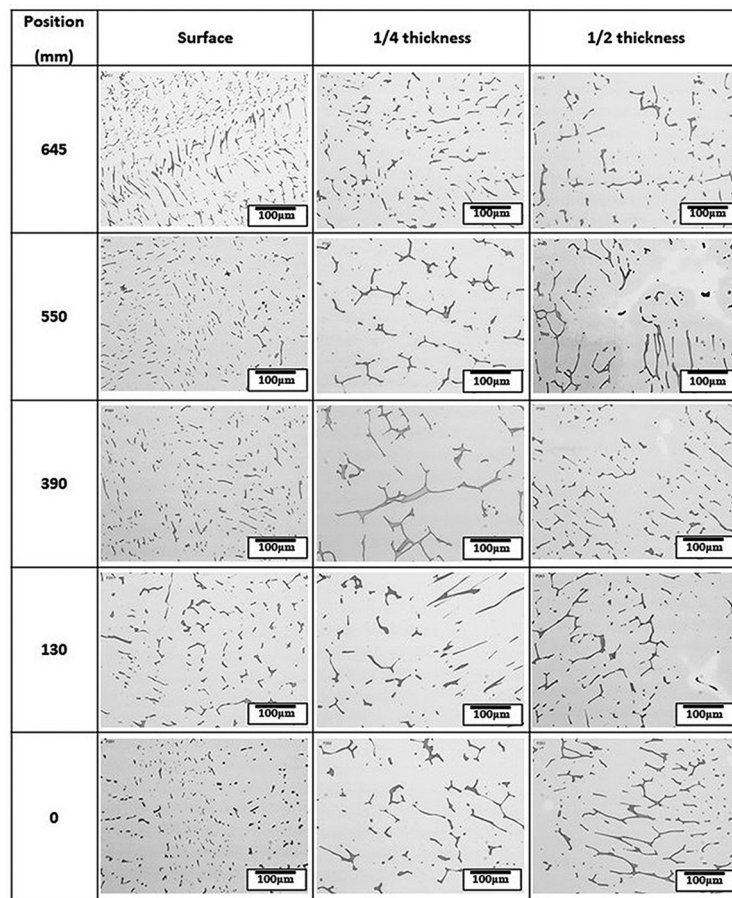


Figure 3 - Micrographs (optical microscopy) of the 15 samples extracted from the continuous casting slab at different distances from the center along the slab width (left) and from the slab surface along its thickness (top). The delta ferrite content of these samples was measured by quantitative metallography (measurement of area fractions of delta ferrite) and by the magnetic method (feritscope). Etchant: NaOH electrolytic.

The decrease in delta ferrite content at the center of the slab was justified by Kim *et al.* (1995) as a result of the macrosegregation of elements to the slab center, changing the local average composition

and the ratio Cr_{eq}/Ni_{eq} to a value lower than 1.5. In this case, the solidification mode would change from FA to AF, which begins with the formation of austenite dendrites that eventually transforms to

ferrite. This is a completely different solidification mode, which could result in a completely different delta ferrite content, changing the tendency observed in the remaining slab.

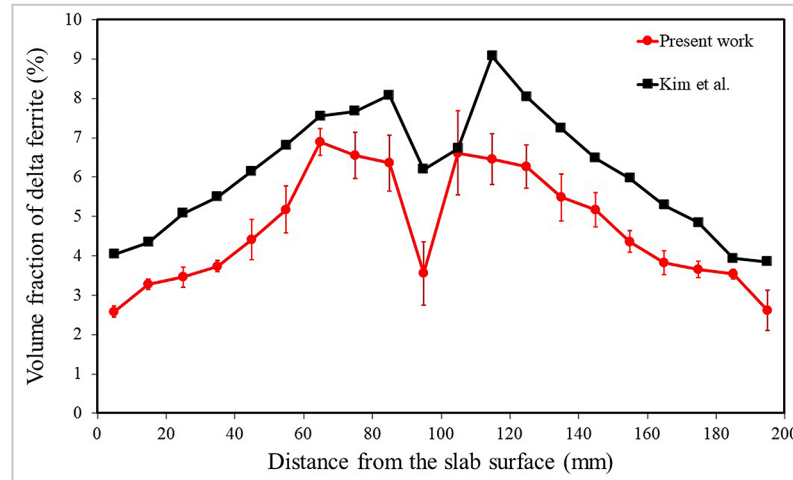


Figure 4 - Volume fraction of delta ferrite measured with the magnetic method (feritscope) at several spots separated by 10 mm as a function of the distance from the as-cast slab surface in sample "A" (Figure 1). The standard deviation bars are also indicated.

To investigate the existence of macrosegregation of elements in the present as-cast slab, chemical analysis was carried out for the fifteen samples indicated in Figure 1. Concentrations of all the elements shown in Table 1, measured by X-ray fluorescence spectroscopy and optical emission spectroscopy, were not significantly different considering the measurement uncertainty, suggesting that macrosegregation was absent. Consequently, the explanation proposed by Kim *et al.* (1995) of the change of solidifica-

tion mode because of the macrosegregation of elements at the slab center does not seem to apply to the presently studied slab.

The only element that exhibited a concentration variation along the slab thickness above the measurement uncertainty (0.002 wt.%) was N (Table 2). This variation, however, was not consistent at the different positions along the slab width, displaying an increase but also a decrease in N concentration depending on the specific location along the width. Consequently, it was not possible

to establish a direct relationship between the N content and the lower delta ferrite content at the slab center. On the other hand, the sample with the lowest N concentration is located at 550 mm from the slab center (along the width) and at 1/2 thickness from the surface. This sample also corresponds to the ferrite peak at 1/2 thickness and can be related to the triangular zone in which columnar dendrites meet. This ferrite peak at the 1/2 slab thickness near the triangular zone was also reported for a Fe-Cr-Mn alloy

Table 2 - Delta ferrite content (vol. %) and nitrogen concentration (N) of the fifteen samples extracted from different distances to the slab center along the slab width (width position) and to the slab surface along the slab thickness (thickness position). The measurement uncertainty for N concentration is 0.002 (wt.%).

Width position (mm)	Thickness position	Delta ferrite (%)	N (wt.%)
645	Surface	4.4	0.041
645	1/4 Thickness	4.1	0.042
645	1/2 Thickness	2.8	0.042
550	Surface	2.4	0.041
550	1/4 Thickness	5.1	0.046
550	1/2 Thickness	4.7	0.037
390	Surface	3.0	0.040
390	1/4 Thickness	5.2	0.041
390	1/2 Thickness	3.2	0.042
130	Surface	3.4	0.041
130	1/4 Thickness	4.5	0.041
130	1/2 Thickness	3.3	0.040
0	Surface	2.6	0.041
0	1/4 Thickness	4.8	0.039
0	1/2 Thickness	4.6	0.039

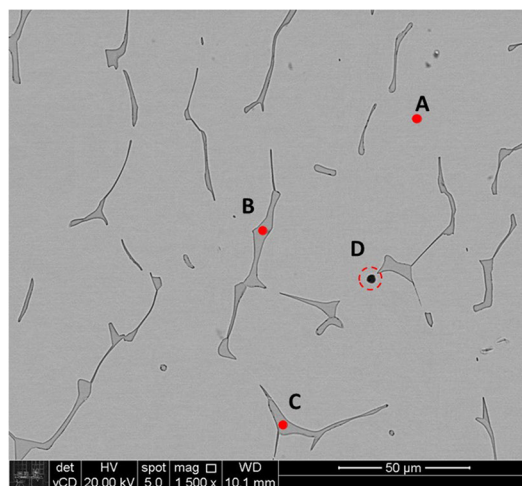
and was associated with the enrichment of carbon and sulfur (Chen & Cheng, 2017).

In Figure 5, the microanalyses with EDS at four spots in the microstructure show the presence of Ca and O in the ferrite phase. The element Ca is added during the desulfurization treatment of the steel melt, whereas the presence of O might be related to the preferential nucleation of ferrite on Ca enriched oxides, which were also observed in the samples. The Si and Cr enrichment in the delta ferrite and Ni

enrichment in the austenite matrix were also observed, as expected.

During the first hot-rolling pass of the as-cast slab at 1100°C, the amount of delta ferrite decreased from values in the range between 2.4 and 6.9% (measured with the feritscope) down to values between 0.7 and 1.4%, as shown in Figure 6. Measurements of delta ferrite fractions using optical microscopy (OM) and area fractions (quantitative metallography) display a pattern similar to that of the magnetic

measurements. The diffraction pattern of a sample from the plate center in Figure 6 is given in Figure 7, displaying the main diffraction lines of ferrite and austenite, which confirms the presence of these phases. After the second hot-rolling pass, delta ferrite contents decreased to values between 0.4 and 1.1%. The lower reduction of ferrite content after this second hot-rolling pass might be related to a lower hot-rolling temperature because the plate did not return to the furnace after the first hot-rolling pass.



Element	Weight(wt.%)			
	A	B	C	D
O	0.84	2.81	3.28	27.88
Si	0.28	0.58	0.62	13.71
Cr	19.43	25.53	24.91	8.21
Mn	1.20	1.04	1.02	6.44
Ni	6.29	3.18	3.09	1.08
Ca	-	0.41	0.41	8.16
Mg	-	-	-	6.24
Al	-	-	-	5.84
Ti	-	-	-	2.04

Figure 5 - Micrograph (scanning electron microscopy) of the sample located at ½ thickness from the slab surface and at 550 mm from the as-cast slab center along its width. Microanalysis with EDS of spots A, B, C and D are also given.

Therefore, less diffusion occurred, causing less ferrite-to-austenite transformation. The reduction in delta ferrite contents during the first and second hot-rolling passes suggests that the $\delta \rightarrow \gamma$ solid-state transformation occurred and changed the microstructure towards the equilibrium predictions of the ThermoCalc® simulation (completely austenitic microstructure). The relatively high rolling temperatures increase the diffusion

coefficient of elements, and the rolling deformation decreases the distance between delta ferrite precipitates, which accelerates the delta ferrite transformation to austenite (Martin & Doherty, 1976). The subsequent solution heat-treating at the minimum temperature of 1040°C, as suggested by the ASTM A480/A480M standard procedure for stainless steel sheet (coil), caused a further decrease in delta ferrite to values between 0.3 to 0.5%. The

significant decrease in delta ferrite content and the presence of delta ferrite stringers (Figure 8) during solution heat-treating confirms the importance of this processing step and its temperature. A clear band with lower ferrite content is evident at ½ thickness from the sheet surface, indicating that the “M type” ferrite distribution can be observed from the continuous cast slab up to the final hot-rolled and solution heat-treated steel.

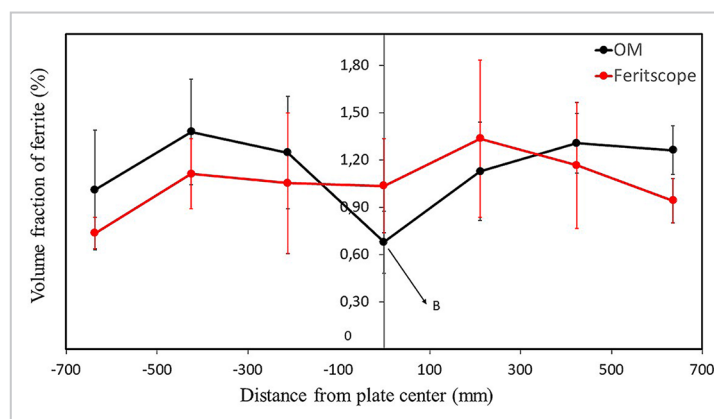


Figure 6 - Volume fractions of delta ferrite measured with the feritscope and optical microscope (OM) using the area fraction (quantitative metallography) as a function of the distance from the center of the plate (after first hot-rolling pass), along its width. Samples were located between ¼ and ½ thickness from the plate surface.

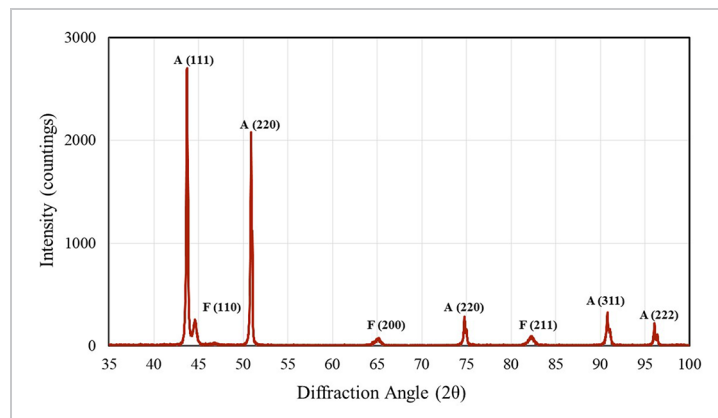


Figure 7 - Diffraction pattern of sample B from Figure 6 obtained with Cu-K α radiation, showing the main diffraction lines of austenite (A) and ferrite (F).

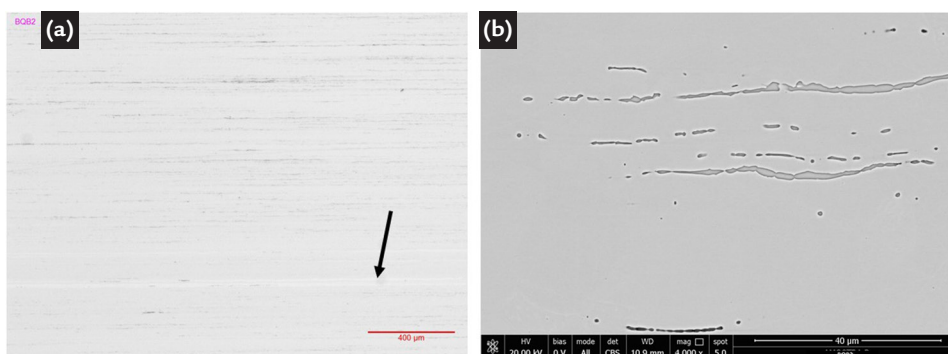


Figure 8 - Microstructures of a sample subjected to the solution heat-treating (commercial condition of the coil): (a) optical microscopy and (b) scanning electron microscopy. Arrow indicates the clear ferrite band at $\frac{1}{2}$ thickness. Etchant: NaOH electrolytic.

4. Conclusion

The microstructural evolution along the production route of an industrial heat of 80 tons of 304 stainless steel was studied. Samples were extracted after the following processing steps: continuous casting (slab), first and second hot-rolling pass, and solution-heat-treating (coil). The microstructures of the samples were analyzed with different characterization techniques, enabling important conclusions. The volume fractions of delta ferrite in the as-cast slab varies between 2.44 and 6.89% in an austenitic matrix. This dual-phase microstructure agrees with the FA solidification mode ($L \rightarrow L + \delta \rightarrow L + \delta + \gamma \rightarrow \gamma + \delta$) predicted for the ratio of $Cr_{eq}/Ni_{eq} = 1.89$ and by

Thermocalc[®] simulations (equilibrium conditions) at the end of solidification. Nevertheless, it disagrees with the Thermocalc[®] simulation for the temperature of 1100 °C, which predicts a completely austenitic microstructure, indicating that the slab processing conditions do not allow thermodynamic equilibrium. The delta ferrite content in the as-cast slab varies from the minimum value of approximately 2.4% at the slab surfaces, increases to 6.9% at about 80 mm from each surface and decreases to approximately 3% at the slab center. This volume fraction profile is in close agreement with that reported by Kim *et al.* (1995) for a similar slab. The delta ferrite content in the as-cast slab decreases to values in the range of 0.7 and

1.4% after the first hot-rolling pass, then to values in the range between 0.4 and 1.1% after the second hot-rolling pass, and finally to values between 0.3 and 0.5% after solution heat-treating (coil). It was verified that the “M type” ferrite distribution observed along the slab thickness persists after the first and second rolling-pass, and after the solution heat-treating. The diffraction pattern of a sample extracted from the slab after the first hot-rolling pass displays the diffraction lines of both ferrite and austenite, as expected. Microanalyses with the energy dispersive spectroscopy (EDS) indicate the existence of Ca and O at some spots within the delta ferrite, which might be due to the preferential nucleation of ferrite on Ca oxide inclusions.

Acknowledgements

The authors thank the support from Aperam South America, Aperam

Services & Solutions, and from the post-graduation program in Metallurgical

and Materials Engineering of the Escola Politécnica da Universidade de São Paulo.

References

- BALDISSIN, D.; PALUMBO, M., BATTEZZATI, L. Modelling and experiments of solidification of AISI 304. *La Metallurgia Italiana*, v. 99, issue 6, p. 25-32, 2007.
CHEN, C.; CHENG, G. Delta-ferrite distribution in a continuous casting slab of Fe-Cr-Mn austenitic stainless

- steel. *Metallurgical and Materials Transactions B*, v. 48B, p 2324-2333, 2017.
- DANTZIG, J. A.; RAPPAZ, M. *Solidification*. Lausanne, EPFL Press, 2009.
- FREDRIKSSON, H. The solidification sequence in an 18-8 stainless steel, investigated by directional solidification. *Metallurgical Transactions*, v. 3, nov., p. 2991-2997, 1972.
- FU, J. W.; YANG, Y. S.; GUO, J. J.; TONG, W. H. Effect of cooling rate on solidification microstructures in AISI 304 stainless steel. *Materials Science and Technology*, v. 24, issue 8, p. 941-944, 2008.
- FUKUMOTO, S.; IWASAKI, Y.; MOTOMURA, H.; FUKUDA, Y. Dissolution behavior of δ -ferrite in continuously cast slabs of SUS304 during heat treatment. *ISIJ International*, v. 52, n. 1, p. 74-79, 2012.
- KIM, S. H.; MOON, H. K., KANG, T.; LEE, C. S. Dissolution kinetics of delta ferrite in AISI 304 stainless steel produced by strip casting process. *Materials Science and Engineering*, v. A356, p. 390-398, 2003.
- KIM, S. K.; SHIN, Y. K.; KIM, N. J. Distribution of delta ferrite content in continuously cast type 304 stainless steel slabs. *Ironmaking and Steelmaking*, v. 22, n. 4, 1995.
- MARTIN, J. W.; DOHERTY, R. D. *Stability of microstructure in metallic systems*. Cambridge(UK): Cambridge University Press, 1976. p. 28-34.
- MARTORANO, M. A.; FAZZIOLI, C. T.; PADILHA, A. F. Predicting delta ferrite content in stainless steel castings. *ISIJ International*, v. 52, n. 6, p. 1054-1065, 2012.
- OKAMOTO, T.; KISHITAKE, K.; MURAKAMI, K. Solidification structure and segregation in iron-chromium-nickel alloys. *Transactions of the Iron and Steel Institute of Japan*, v. 21, issue 9, p. 641-648, 1981.
- PADILHA, A. F. Aços inoxidáveis: histórico e desenvolvimento. In: BOTT, I (ed.). *Aços: perspectivas para os próximos 10 anos*. Rede Aços, Rio de Janeiro, p. 129-138, nov. 2002.
- PADILHA, A. F.; PLAUT, R. L.; RIOS, P. R. Stainless steel heat treatment. In: TOTTEN, G. E. (ed.). *Steel heat treatment handbook*. 2. ed. Boca Raton, FL, USA: CRC Press-Taylor & Francis, 2007. cap. 12, p. 695-739.
- PADILHA, A. F.; RIOS, P. R. Decomposition of austenite in austenitic stainless steels. *ISIJ International (Japan)*, v. 42, n. 4, p. 325-337, 2002.
- RAJASEKHAR, C. S.; HARENDRANATH, R.; RAMAN, S.; KULKARNI, S. D. Microstructural evolution during solidification of austenitic stainless steel weld metals: a color metallographic and electron microprobe analysis study. *Materials Characterization*, v. 38, n. 2, p. 53-65, 1997.
- REZAYAT, M.; MIRZADEH, H.; NAMDAR, M.; PARSA, M. H. Unraveling the effect of thermomechanical treatment on the dissolution of delta ferrite in austenitic stainless steels. *Metallurgical and Materials Transactions A*, v. 47, n. 2, p. 641-648, fev. 2016.
- SUUTALA, N.; TAKALO, T.; MOISIO, T. Ferritic-Austenitic solidification mode in austenitic stainless steel welds. *Metallurgical Transactions A*, v. 11, n. 5, p. 717-725, 1980.
- ZANGAR, T.; SADEGHI, F.; KIM, J. W.; LEE, J. S.; HEO, Y-U; YIM, C. H. Kinetic model to investigate the effect of cooling rate on δ -Ferrite behavior and its application in continuous casting of AISI 304 stainless steel. *Met. Mater. Int.* 2021. Available at: <https://doi.org/10.1007/s12540-021-01118-z>.

Received: 7 January 2020 - Accepted: 30 August 2022.

